J. Cent. South Univ. (2020) 27: 3053−3062
DOI: https://doi.org/10.1007/s11771-020-4528-2

Springer

Strength and energy exchange of deep sandstone under high hydraulic conditions

LI Fei(李飞)[1, 2], YOU Shuang(由爽)[1, 2], JI Hong-guang(纪洪广)[1, 2],
ELMO Davide[3], WANG Hong-tao(王洪涛)[1, 2]

1. Beijing Key Laboratory of Urban Underground Space Engineering, University of Science and Technology Beijing, Beijing 100083, China;
2. School of Civil and Resource Engineering, University of Science and Technology Beijing, Beijing 100083, China;
3. Institute of Mining Engineering, University of British Columbia, BC V6T 1Z4, Canada

Abstract: To investigate the influence of confining pressure and pore water pressure on strength characteristics, energy storage state and energy release intensity at peak failure of deep sandstone, a series of triaxial compression tests under hydraulic coupling conditions are carried out. By analyzing the process of rock deformation and failure, the stress thresholds of the rock are obtained. The change trend of total energy density, elastic energy density and dissipated energy density of deep sandstone in the pre-peak stage is obtained by the graphical integration method. By comparing the dynamic energy storage level of rocks under different confining pressures, the influence of pore water pressure on the energy dissipation at stress thresholds of crack closure stress, crack initiation stress, crack damage stress and peak stress is analyzed. Based on the ratio of pre-peak total energy density to post-peak total energy density, the interaction mechanism of confining pressure and pore water pressure for the rock burst proneness of deep sandstone is studied. The experimental results show that the peak stress of sandstone increases with the increase of confining pressure, while the existence of pore water pressure can weaken the peak stress of sandstone. In the stress stage from crack closure stress to peak stress, the dynamic energy storage level of rock presents a trend of the inverse “check mark”. Meanwhile, the larger the confining pressure, the higher the energy storage level of rock. However, the pore water pressure increases the degree of energy dissipation of rock and reduces the energy storage capacity of rock, and the degree of dissipation is linear with pore water pressure. The increase of confining pressure aggravates the instability and failure of deep sandstone, while pore water pressure has the opposite effect. The research results will provide necessary data support for the stability analysis of rock mass excavation in sandstone stratum under high stress and high pore water pressure.

Key words: deep sandstone; high hydraulic pressure; mechanical characteristics; energy storage; rock burst proneness

Cite this article as: LI Fei, YOU Shuang, JI Hong-guang, ELMO Davide, WANG Hong-tao. Strength and energy exchange of deep sandstone under high hydraulic conditions [J]. Journal of Central South University, 2020, 27(10): 3053−3062. DOI: https://doi.org/10.1007/s11771-020-4528-2.

1 Introduction

At present, with the rapid development of global economy, there is a major contradiction between the increasing demand for resources and the rapid depletion of global shallow resources, and the development of deep resources has become the

Foundation item: Project(2016YFC0600801) supported by the National Key Research Development Program of China; Project(51774021) supported by the National Natural Science Foundation of China; Project(2019SDZY05) supported by the Major Scientific and Technological Innovation Project of Shandong Province, China
Received date: 2020-06-15; **Accepted date:** 2020-08-27
Corresponding author: YOU Shuang, PhD, Associate Professor; Tel: +86-10-62333867; E-mail: youshuang@ustb.edu.cn; ORCID: https://orcid.org/0000-0002-3158-3371

only effective solution [1]. However, with the increasing of mining depth, there are many special and unique engineering problems in deep rock engineering, such as violent rock burst, large deformation of deep chamber, serious water inrush accidents [2−5], because the rock mass of deep engineering is in a complex stress environment of high ground stress, high pore water pressure, high rock temperature and strong mining disturbance [6]. High stress in three directions leads to a large amount of deformation energy stored in the deep rock mass, and the excavation disturbance makes the internal energy of the high energy storage rock mass easy to release, resulting in serious engineering disasters and economic losses [7, 8]. High pore water pressure also affects the deep rock mass, which is conducive to the development and connection of the original defects in the rock mass [9], significantly weakening the strength indexes of the rock, leading to water inrush accidents in the process of deep mining.

In the past, researchers mainly focused on a single mechanical factor to study the mechanical characteristics of the rock samples, and simulated different stress conditions by changing the stress path of the tests. The early tests simply increased the confining pressure and found that the strength of the rock samples increased correspondingly, indicating that the rock samples is a kind of pressure sensitive material [10]. Since then, some researchers obtained the mechanical properties of engineering rock mass under different stress environment through a variety of unconventional mechanical tests [11−13], such as cyclic loading and unloading test, monocycling test, creep test. At present, scholars have gradually paid attention to the influence of intermediate principal stress on the mechanical properties of rock samples, and carried out true triaxial compression test to study the factor [14, 15]. In this paper, the intermediate principal stress and minimum principal stress are unified into confining pressure by averaging method, and the pseudo triaxial compression test is used to study the mechanical properties and energy dissipation characteristics of the rock samples. With the current engineering geological conditions becoming more and more complex, more researchers begin to realize that pore water pressure has an influence on the rock samples, and the research of the rock samples mechanical properties under the hydraulic coupling has become the frontier topic of current research. WANG et al [16] studied the mechanical properties and permeability of coal mine sandstone and limestone under hydraulic coupling, and revealed the differences of mechanical properties and permeability before and after rock failure. ZHOU et al [17] conducted conventional triaxial compression tests and hydraulic coupling tests on Beishan granite to study the mechanical behavior of the failure process. LI et al [18] elucidated the stress−strain relationship of brittle rocks containing microcracks under the effect of confining pressure, water pressure and axial stress. However, the coupling mechanism of high confining pressure and high pore water pressure and the mechanical response of deep rock under its action are unclear. The mechanical behavior of deep rock mass is nonlinear due to the combined effect of multiple fields, which leads to the failure of rock failure analysis based on stress criterion.

The failure process of the rock samples is essentially the result of energy driven, the energy evolution and distribution tendency of the rock samples in different loading stages are different [19, 20]. It is more scientific to explain the deformation and failure of the rock samples in different loading stages from the perspective of energy, and more research results have appeared [21−25]. HOU et al [21] obtained the mechanical properties and energy evolution characteristics of shales through uniaxial compression tests. LI et al [22] conducted triaxial loading and unloading tests with different initial confining pressures, and obtained the change trend of energy index of granite during deformation and failure. GONG et al [25] used the energy analysis method to study the failure mechanism of rocks, and obtained the energy distribution mode during the tension-type failure process of marble. However, few achievements have been made to study the energy evolution process of deep rock under the coupling of high confining pressure and high pore water pressure. Moreover, the impact of pore water pressure on energy dissipation is unclearly stated.

In this paper, the deep sandstones of different depths were selected as the research object. Through the triaxial compression tests under different confining pressures and pore water

pressures, the stress−strain curves of the deep sandstone were obtained. Firstly, the stress thresholds were obtained, and the strength characteristics and mechanical behavior and of rock sample were analyzed. Then the trend of energy storage level of rock sample in the stress stage from crack closure stress to peak stress was analyzed, and the energy dissipation characteristics of the rock samples at different stress stages were obtained. Finally, the relationship between rock burst proneness and stress conditions was studied and the influence of confining pressure and pore water pressure on the rock samples failure tendency was revealed.

2 Experimental study

2.1 Rock samples and preparation

The rock samples used in the test were taken from Yuncheng Coal Mine, Shandong Province, China. The depths of rock samples were 700, 800 and 900 m. The component analysis results show that the rock samples contain more than 50% quartz sand, a certain amount of clay mineral fillers and a small amount of other minerals, so they are identified as quartz sandstone. The average densities of 700, 800 and 900 m rock samples are 2.38, 2.54 and 2.63 g/cm^3, respectively. The average porosity of 700 m, 800 m, and 900 m rock samples are 7.38%, 5.35%, and 3.82%, respectively. The sandstone cores were processed into standard cylindrical rock samples with diameter of 50 mm and height of 100 mm, and the surface of the samples was free of obvious defects (Figure 1). The non-parallelism of the parallel end faces of the rock samples and the deviation between the nonparallel end faces and the axial meet the standards of the International Society for Rock Mechanics (ISRM) standard. The rock samples of the same depth with similar longitudinal wave velocity were selected by ultrasonic testing, and the error of subsequent mechanical tests can reduce. For the interpretation of rock sample number, “C” and “H” represented the rock samples under the conventional condition and the hydraulic coupling condition, respectively; “700”, “800” and “900” represented the sample depths were 700, 800 and 900 m, respectively.

2.2 Test instrument and test schemes

The stress loading system used in the tests is TAW-2000 electrohydraulic servocontrolled triaxial test machine. The maximum confining pressure is 100 MPa, the maximum pore water pressure is 60 MPa and the maximum axial load is 2000 kN. The axial strain and the radial strain can be measured by the corresponding extensometer. The measurement range of rock sample axial deformation is 0−5 mm, and the radial deformation is 0−3 mm, the measurement resolution is 1×10^{-4} mm, and the measurement accuracy is ±1%, which meets the accuracy requirements of the study.

As shown in Figure 2, the confining pressure is loaded to the predetermined value of the experiment, and then the pore water pressure is loaded to the

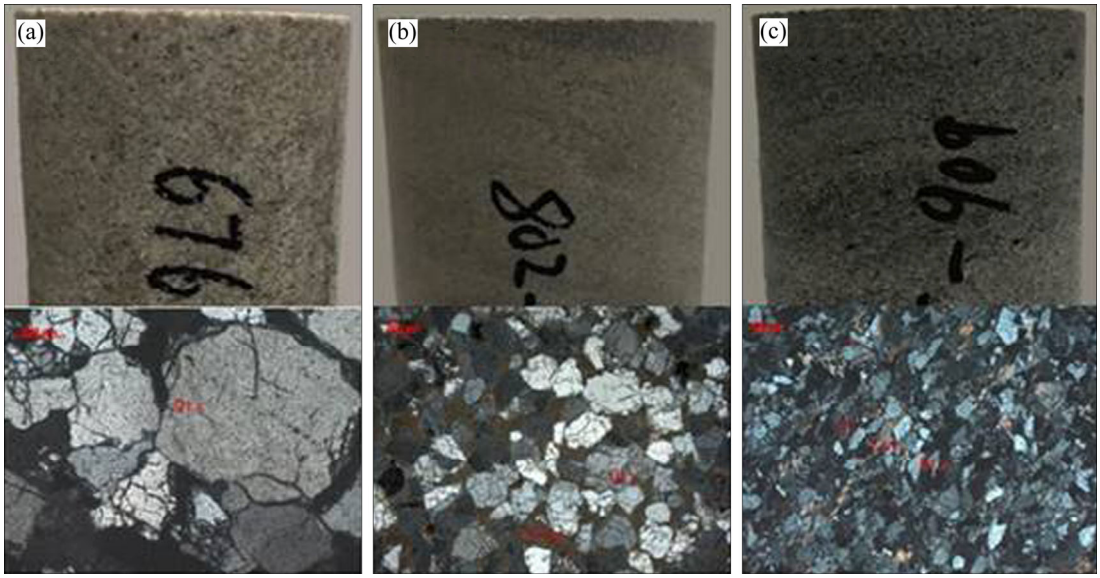

Figure 1 Samples and microstructures: (a) 700 m; (b) 800 m; (c) 900 m

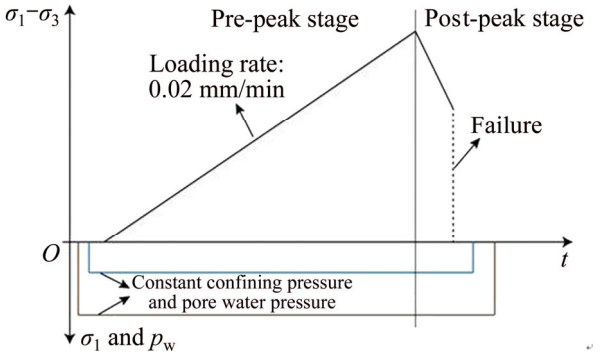

Figure 2 Diagram of stress path

predetermined value after the confining pressure remains stable, and finally the axial stress with loading rate of 0.02 mm/min is loaded until the rock sample failure.

According to monitoring data of the borehole strain and pore water pressure in Yuncheng Coal Mine, it is learned the values of confining pressure σ_3 and pore water pressure p_w of sandstone in the depth of 700, 800 and 900 m. The sample number and its experimental parameter settings are shown in Table 1.

Table 1 Stress conditions of mechanical test

Sample number	σ_3/MPa	p_w/MPa
C-700	15	0
C-800	17	0
C-900	19	0
H-700	15	7
H-800	17	8
H-900	19	9

3 Tests results and their analysis

3.1 Calculation of stress thresholds and division of stress−strain stages

The stress−strain characteristics of deep sandstones are shown in Figure 3. It can be found that the rock samples have no residual stress under the conventional condition. Under the hydraulic coupling condition, the rock samples have residual stress under low stress and no residual stress under high stress. The elastic modulus of 700, 800 and 900 m rock samples are 28.08, 22.57 and 35.72 GPa, respectively. The Poisson ratios of rock samples are 0.27, 0.26 and 0.31, respectively.

The relationship between peak stress and

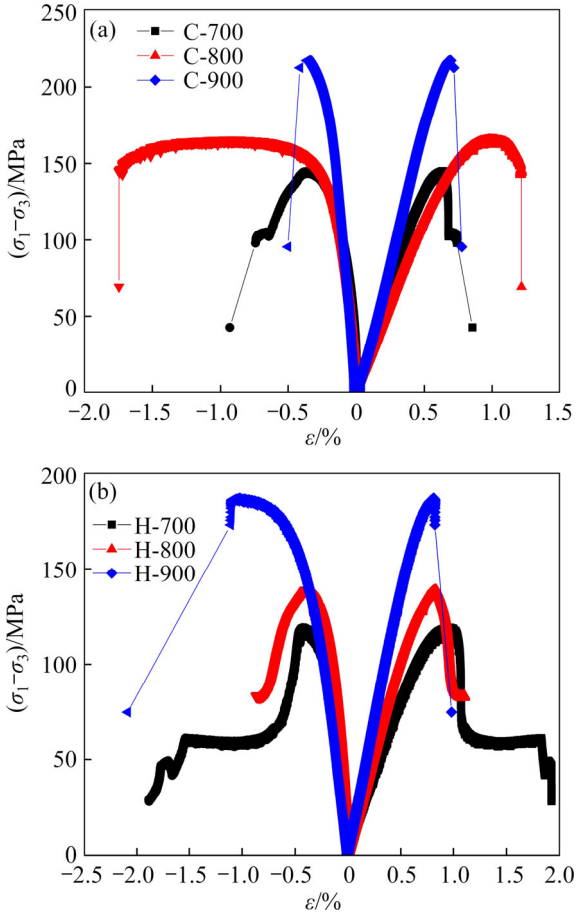

Figure 3 Stress−strain curves of deep sandstones: (a) Under conventional condition; (b) Under hydraulic coupling condition

confining pressure is shown in Figure 4(a). It is found that the peak stress of sandstone increases with the increase of effective confining pressure, because the confining pressure hinders the development of internal cracks and increases the strength of the rock. And the rock samples under the conventional condition shows higher peak stress at the same confining pressure level than under the hydraulic coupling condition, which indicates that the pore water pressure can promote the development of cracks and weaken the strength characteristics of the rock sample.

Equation (1) is used to obtain the fitting relationship between pore water pressure and the loss range of the peak stress, as shown in Figure 4(b). It is found that with the increase of pore water pressure, the decrease range of peak stress gradually decreases. This is because both confining pressure and pore water pressure increase in triaxial compression test, and the increase range of confining pressure (2 MPa) is greater than that of

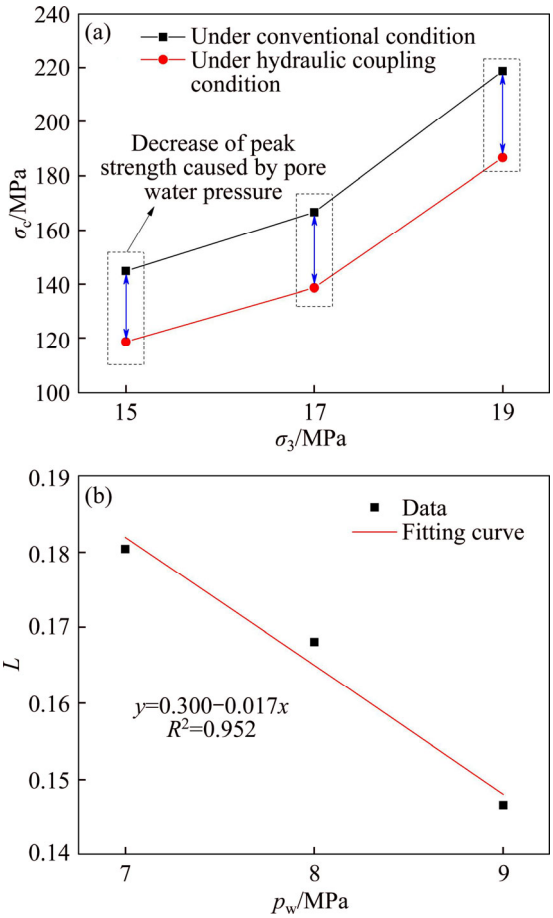

Figure 4 Relationship between stress conditions and peak stress: (a) Impact of confining pressure on peak stress; (b) Impact of pore water pressure on loss range of peak stress

pore water pressure (1 MPa), so the influence of pore water pressure on strength characteristics of rock sample is weakened.

$$L=\frac{\sigma_c^c-\sigma_c^h}{\sigma_c^c} \tag{1}$$

where L is the loss range of the peak stress; σ_c^c is the peak stress of rock sample under the conventional condition; σ_c^h is the peak stress of rock sample under the hydraulic coupling condition.

The brittleness index of the rock sample at the post-peak stage is obtained by the stress dropping rate:

$$n=\frac{\sigma_p-\sigma_r}{\varepsilon_r-\varepsilon_p} \tag{2}$$

where n is the stress dropping rate.

As shown in Figure 5, with the increase of confining pressure, the rate of stress decrease gradually accelerates, the brittleness of the rock

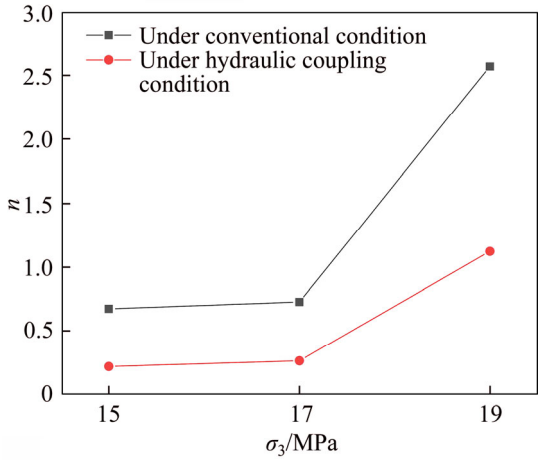

Figure 5 Variation of stress dropping rate

samples becomes more obvious, the energy release becomes more intense [26], and the structure of sample becomes unstable gradually. In addition, pore water pressure increases the energy dissipation in the pre-peak stage, reduces the energy release after peak failure, slows down the stress dropping rate, and decreases the impact on structure.

In the test, the mechanical behavior of the rock sample in the post-peak stage is not only affected by the confining pressure, but also affected by the pore water pressure. Under the conventional condition, the sample stress drops in the post-peak stage without a residual stage. This is because the structure of the rock sample is more compact due to the increase in confining pressure. The energy storage level before the peak is increased, and the internal energy of the rock sample is released after the peak failure occurs, which impacts the stability of structure. After the peak failure of the sandstone under hydraulic coupling, it still has a certain bearing capacity. The pore water pressure can increase the energy dissipation of the rock sample before the peak, which will reduce the intensity of energy release and reduce the impact on the structure. It should be noted that H-9 shows no residual stress. This is because the sample is not only affected by high pore water pressure, but also limited by high confining pressure. The high confining pressure allows the rock sample to store more energy in the pre-peak stage, and the energy dissipation caused by pore water pressure can only reduce the energy storage level of the rock sample to a limited extent, causing the rock sample to release more energy than the energy that its structure can carry. The energy storage

characteristics and energy release intensity for rock sample will be explained in detail later.

3.2 Characteristics of pre-peak stage energy storage level and energy dissipation at stress thresholds

It is assumed that there is no heat transfer between the sandstone samples and the outside during the stress loading period, so the total energy density (U) generated by the rock samples under the external force is all transformed into the elastic energy density (U_e) and the dissipated energy density (U_d). The elastic energy density (U_e) is stored in the sandstone samples, which is released immediately after the external load is removed, which belongs to the bidirectional reversible energy, while the dissipated energy density (U_d) is used for the defect development and plastic deformation in the rock samples, which is irreversible energy. Each energy density is calculated as follows:

$$U=\int_0^{\varepsilon_1}\sigma_1 \mathrm{d}\varepsilon_1+2\int_0^{\varepsilon_3}\sigma_3 \mathrm{d}\varepsilon_3 \tag{3}$$

$$U_e=\frac{1}{2E_u}\left[\sigma_1^2+2\sigma_3^2-2\nu_i\left(2\sigma_1\sigma_3+\sigma_3^2\right)\right] \tag{4}$$

$$U_d=U-U_e \tag{5}$$

where U is the total energy density; U_e is the elastic energy density; U_d is the dissipated energy density; E_u is the unloading elastic module. It should be noted that the initial elastic modulus is generally used instead of the unloading elastic modulus.

As shown in Figure 6, taking C-8 as an example, the evolution tendency of the energy density index in the pre-peak phase of the rock

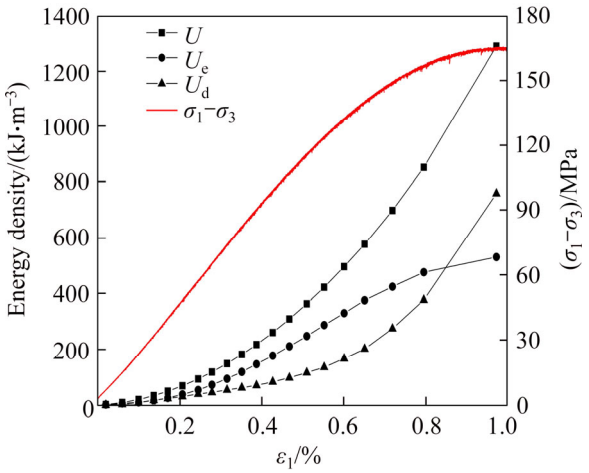

Figure 6 Variation of energy density and axial deviatoric stress with axial strain

sample is obtained. Because the stress loading system continuously does work on the rock sample, each energy density generally shows an upward trend in the pre-peak stage.

Each energy density index of the rock sample is increasing during the pre-peak stage, and the ratio of elastic energy density to total energy density is a reflection of the energy storage capacity of the rock sample under a certain stress level or strain level. As the relative strain level increases, the internal deformation of the rock sample changes, and the energy storage characteristics of the rock sample also change dynamically. Therefore, the phenomenon is called the dynamic energy storage level of the rock sample. The formula is as follows:

$$S=\frac{U_e}{U} \tag{6}$$

where S is the energy storage level.

As shown in Figure 7(a), the energy storage levels between the crack closure stress and the peak stress of the rock samples under different confining pressures generally increase first and then decrease as the axial deviatoric stress increases. This is because when the axial deviatoric stress exceeds the crack closure stress, the rock sample enters the elastic stage, and the internal structure of the rock sample is increasingly compact, and its energy storage capacity is constantly enhanced. The proportion of energy input from the outside into the energy stored in the rock sample is increasing. When the axial deviatoric stress reaches the crack initiation stress, microcrack begins to appear inside the rock sample, and the increase rate of the energy storage level of the rock sample decreases. As the axial deviatoric stress continues to increase, when the crack damage stress is exceeded, the rock sample enters the expansion stage, the internal cracks rapidly develop and penetrate, and the energy storage level begins to decline. It should be noted that there are different degrees of porous in different rock samples, which will interfere with the energy accumulation in the compaction stage, and it is easy to form a macro section near the peak failure. Therefore, the final stage of the curve in Figure 10(a) violates the overall tendency.

Equation (7) is used to analyze the effect of pore water pressure on the rock sample energy dissipation at various stress thresholds, as shown in Figure 7(b). From the stage of crack closure stress to crack damage stress, the degree of energy

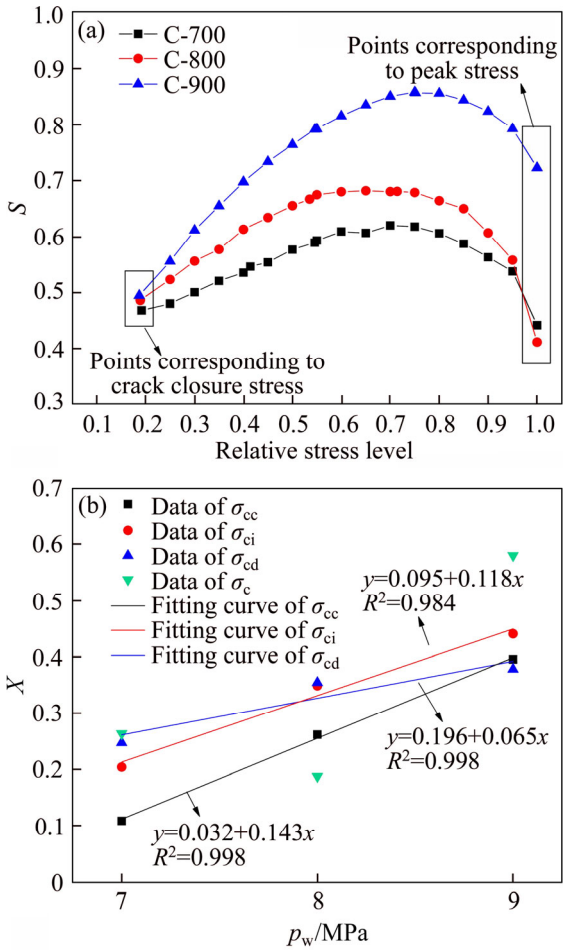

Figure 7 Relationship between stress conditions and energy transformation of rock sample: (a) Impact of confining stress on energy storage level of rock sample from crack closure stress to peak stress; (b) Impact of pore water pressure on reduction range of energy storage level at stress thresholds

dissipation increases linearly with the increase of pore water pressure. This is because the number of cracks in the rock sample increases steadily with the increase of axial deviatoric stress in the stage and pore water pressure can promote cracks growth. Therefore, the influence of pore water pressure on energy dissipation in rock sample increases gradually. Reaching the expansion stage, the cracks develop unsteadily, and the irregular seepage channel formed by the internal primary fracture of the rock sample leads to the significant reduction of the energy storage level of the rock sample [27], which is also reflected in Figure 7(a).

$$X = \frac{S_i^{\mathrm{c}} - S_i^{\mathrm{h}}}{S_i^{\mathrm{c}}} \tag{7}$$

where X is reduction range of energy storage level at stress thresholds; S_i^{c} is the energy storage level of rock sample at stress threshold i under the conventional condition; S_i^{h} is the energy storage level of rock sample at stress threshold i under the hydraulic coupling condition.

3.3 Effect of confining pressure and pore water pressure on rock burst proneness of deep sandstone

When the rock sample is subjected to continuous axial stress, it absorbs the input energy from the outside continuously in the pre-peak stage. When the axial stress of the rock sample exceeds the limit of its bearing capacity, the internal energy release impacts the overall structure, resulting in the stress dropping phenomenon in the rock sample. The residual energy in the post-peak stage can be obtained by integrating the curves in the post-peak stage, as shown in Figure 8. The evaluation index of the rock burst proneness W_{cf} is calculated as follows [28]:

$$W_{\mathrm{cf}} = \frac{U_1}{U_2} \tag{8}$$

where W_{cf} is the evaluation indexes for the rock burst proneness; U_1 is the total energy density of the rock sample in the pre-peak stage; U_2 is the total energy density of the rock sample in the post-peak stage.

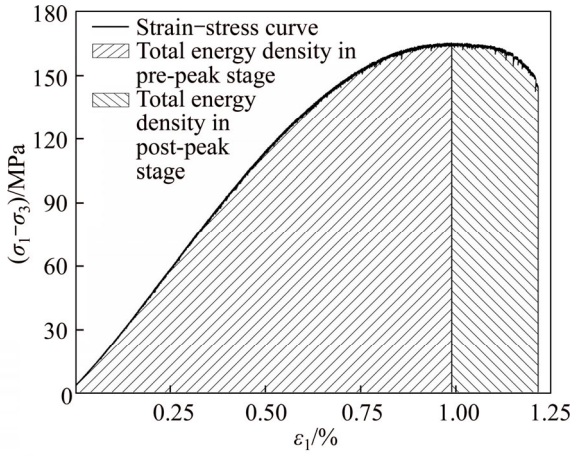

Figure 8 Diagram of total energy density calculation in pre-peak stage and post-peak stage

As shown in Figure 9, the rock burst proneness of the rock samples increases with the increase of confining pressure, because the increase of confining pressure increases the energy absorbed by rock samples in the pre-peak stage. When the rock

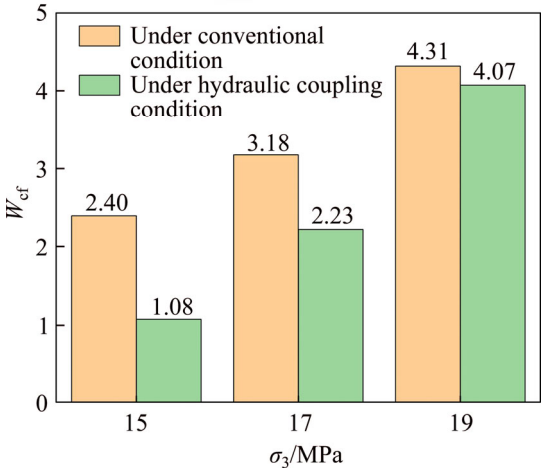

Figure 9 Evaluation indexes for rock burst proneness of rock samples

samples reach the peak stress, the energy release is more intense, and pore water pressure significantly reduces the rock burst proneness of rock samples.

Using Eq. (9) to calculate the weaken value of rock burst proneness under the same confining pressure (Figure 10). With the increase of depth, the confining pressure and pore water pressure increase simultaneously, and the weaken value of rock burst proneness decreases. For the increasing range of confining pressure is greater than that of pore water pressure, and the strengthening effect of confining pressure on rock sample is gradually greater than the weakening effect of pore water pressure on rock sample, leading to the decrease of the weaken value of rock burst proneness.

$$W = W_{cf}^{c} - W_{cf}^{h} \tag{9}$$

where W is the weaken value of the rock burst proneness; W_{cf}^{c} is the rock burst proneness of rock sample under the conventional condition; W_{cf}^{h} is the rock burst proneness of rock sample under the hydraulic coupling condition.

From the engineering point of view, with the increase of rock sample depth, the confining pressure becomes larger and larger, and the rock burst proneness of the surrounding rock is higher and higher, while the pore water pressure will partly reduce the impact energy on the rock mass. When the confining pressure reaches a higher value, that is, when the engineering depth is large, more pore water pressure is needed to reduce the impact of energy release on the structure when the rock mass is damaged.

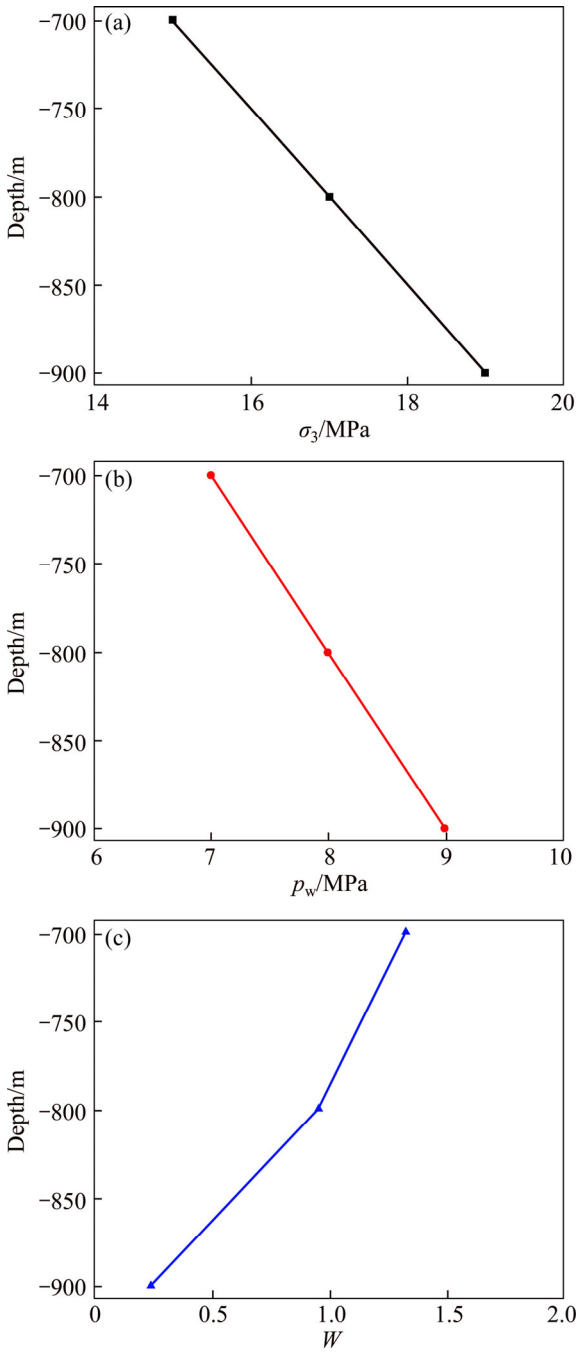

Figure 10 Relationship between weaken value of rock burst proneness and stress environment

4 Conclusions

With the increase of confining pressure level, the internal structure of rock sample becomes compact, the generation of microcracks requires a higher level of axial stress, and its peak stress is correspondingly increased. Water exists in the internal cracks of the rock sample, and pore water pressure can reduce the effective confining pressure, promote the growth and development of

microcracks, and reduce the strength characteristics of rock sample. The energy density indexes of the rock sample in the pre-peak stage gradually increase with the increase of the stress level. The trend of energy storage level of rock sample in the stress stage from crack closure stress to peak stress changes from rising to falling. As the relative position of the stress threshold on the stress curve increases, the number of cracks in the rock sample gradually increases, and eventually through fractures are formed. The effect of pore water pressure on rock sample energy dissipation increases gradually. The confining pressure increases the energy density input from outside in the pre-peak stage and enhances the rock burst proneness level, while pore water pressure will dissipate part of the energy accumulated in the pre-peak stage, thus reducing the rock burst proneness risk.

Contributors

The overarching research goals were developed by LI Fei, YOU Shuang, JI Hong-guang and ELMO Davide. LI Fei and WANG Hong-tao carried out mechanical tests. LI Fei analyzed the data. LI Fei and YOU shuang wrote the paper. All authors replied to reviewers' comments and revised the final version.

Conflicts of interest

LI Fei, YOU Shuang, JI Hong-guang, ELMO Davide and WANG Hong-tao declare that they have no conflict of interest.

References

[1] CAI Mei-feng, BROWN E T. Challenges in the mining and utilization of deep mineral resources [J]. Engineering, 2017, 3(4): 432−433. DOI: 10.1016/ J.ENG.2017.04.027.

[2] FENG Xia-ting, LIU Jian-po, CHEN Bing-rui, XIAO Ya-xun, FENG Guang-liang, ZHANG Feng-peng. Monitoring, warning, and control of rockburst in deep metal mines [J]. Engineering, 2017, 3(4): 538−545. DOI: 10.1016/J.ENG. 2017.04. 013.

[3] KANG Hong-pu. Support technologies for deep and complex roadways in underground coal mines: A review [J]. International Journal of Coal Science & Technology, 2014, 1(3): 261−277. DOI: 10.1007/ s40789-014-0043-0.

[4] CUI Fang-peng, WU Qiang, LIN Yuan-hui, ZENG Yi-fan, ZHANG Ke-li. Damage features and formation mechanism of the strong water inrush disaster at the Daxing Co Mine, Guangdong province, China [J]. Mine Water and the Environment, 2018, 37(2): 346−350. DOI: 10.1007/ s10230-018-0530-4.

[5] LUO Yong, GONG Feng-qiang, LI Xi-bing, WANG Shan-yong. Experimental simulation investigation of influence of depth on spalling characteristics in circular hard rock tunnel [J]. Journal of Central South University, 2020, 27(3): 891−910. DOI: 10.1007/s11771-020-4339-5.

[6] YIN Li-ming, MA Kai, CHEN Jun-tao, XUE Yan-chao, WANG Zi-qi, CUI Bo-qiang. Mechanical model on water inrush assessment related to deep mining above multiple aquifers [J]. Mine Water and the Environment, 2019, 38(4): 827−836. DOI: 10.1007/s10230-019-00623-3.

[7] LI Xi-bing, GONG Feng-qiang, TAO Ming, DONG Long-jun, DU Kun, MA Chun-de, ZHOU Zi-long, YIN Tu-bing. Failure mechanism and coupled static-dynamic loading theory in deep hard rock mining: A review [J]. Journal of Rock Mechanics and Geotechnical Engineering, 2017, 9(4): 767−782. DOI: 10.1016/j.jrmge.2017.04.004.

[8] SI Xue-feng, GONG Feng-qiang. Strength-weakening effect and shear-tension failure mode transformation mechanism of rockburst for fine-grained granite under triaxial unloading compression [J]. International Journal of Rock Mechanics and Mining Sciences, 2020, 131: 104347. DOI: 10.1016/ j.ijrmms.2020.104347.

[9] ZHOU Zhong, YANG Hao, WANG Xiang-can, ZHANG Qi-fang. Fractured rock mass hydraulic fracturing under hydrodynamic and hydrostatic pressure joint action [J]. Journal of Central South University, 2016, 23(10): 2695−2704. DOI: 10.1007/s11771-016-3331-6.

[10] COOKNGW. The failure of rock [J]. International Journal of Rock Mechanics and Mining Sciences & Geomechanics Abstracts, 1965, 2(4): 389−403. DOI: 10.1016/0148-9062(65) 90004-5.

[11] YOU Shuang, JI Hong-guang, ZHANG Zi-jian, ZHANG Cheng-han. Damage evaluation for rock burst proneness of deep hard rock under triaxial cyclic loading [J]. Advances in Civil Engineering, 2018(1): 1−7. DOI: 10.1155/2018/ 8193638.

[12] GONG Feng-qiang, LUO Yong, LI Xi-bing, SI Xue-feng, TAO Ming. Experimental simulation investigation on rockburst induced by spalling failure in deep circular tunnels [J]. Tunnelling and Underground Space Technology, 2018, 81: 413−427. DOI: 10.1016/j.tust.2018.07.035.

[13] ZHANG Yu, XU Wei-ya, GU Jin-jian, WANG Wei. Triaxial creep tests of weak sandstone from fracture zone of high dam foundation [J]. Journal of Central South University, 2013, 20(9): 2528−2536. DOI: 10.1007/s11771-013-1765-7.

[14] FENG Xia-ting, KONG Rui, ZHANG Xi-wei, YANG Cheng-xiang. Experimental study of failure differences in hard rock under true triaxial compression [J]. Rock Mechanics and Rock Engineering, 2019, 52(7): 2109−2122. DOI: 10.1007/s00603-018-1700-1.

[15] SHANG Jun-long. Rupture of veined granite in polyaxial compression: insights from three-dimensional discrete element method modeling [J]. Journal of Geophysical Research, 2020, 125(2): e2019JB019052. DOI: 10.1029/ 2019JB019052.

[16] WANG Lu, LIU Jian-feng, PEI Jian-liang, XU Hui-ning, BIAN Yu. Mechanical and permeability characteristics of

rock under hydro-mechanical coupling conditions [J]. Environmental Earth Sciences, 2015, 73(10): 5987−5996. DOI: 10.1007/ s12665-015-4190-4.

[17] ZHOU Hong-wei, WANG Zi-hui, REN Wei-guang, LIU Ze-lin, LIU Jian-feng. Acoustic emission based mechanical behaviors of Beishan granite under conventional triaxial compression and hydro-mechanical coupling tests [J]. International Journal of Rock Mechanics and Mining Sciences, 2019, 123: 104125. DOI: 10.1016/j.ijrmms.2019.104125.

[18] LI Zhi-hao, XIONG Zi-ming, CHEN Hao-xiang, LU Hao, HUANG Mu, MA Chao, LIU Yi-ming. Analysis of stress-strain relationship of brittle rock containing microcracks under water pressure [J]. Bulletin of Engineering Geology and the Environment, 2020, 79(4): 1909−1918. DOI: 10.1007/s10064-019-01660-6.

[19] XIE He-ping, LI Li-yun, PENG Rui-dong, JU Yang. Energy analysis and criteria for structural failure of rocks [J]. Journal of Rock Mechanics and Geotechnical Engineering, 2009, 1(1): 11−20. DOI: 10.3724/SP.J.1235.2009.00011.

[20] MENG Qing-bin, ZHANG Ming-wei, HAN Li-jun, PU Hai, NIE Tao-yi. Effects of acoustic emission and energy evolution of rock specimens under the uniaxial cyclic loading and unloading compression [J]. Rock Mechanics and Rock Engineering, 2016, 49(10): 3873−3886. DOI: 10.1007/s00603-016-1077-y.

[21] HOU Peng, GAO Feng, YANG Yu-gui, ZHANG Xiang-xiang, ZHANG Zhi-zhen. Effect of the layer orientation on mechanics and energy evolution characteristics of shales under uniaxial loading [J]. International Journal of Mining Science and Technology, 2016, 26(5): 857−862. DOI: 10.1016/ j.ijmst.2016.05.041.

[22] LI Di-yuan, SUN Zhi, XIE Tao, LI Xi-bing, RANJITH P G. Energy evolution characteristics of hard rock during triaxial failure with different loading and unloading paths [J]. Engineering Geology, 2017, 228: 270−281. DOI: 10.1016/j.enggeo.2017.08.006.

[23] PEI Feng, JI Hong-guang, ZHANG Tong-zhao. Energy evolution and mechanical features of granite subjected to triaxial loading-unloading cycles [J]. Advances in Civil Engineering, 2019, 2019(1): 1−11. DOI: 10.1155/2019/9871424.

[24] GONG Feng-qiang, YAN Jing-yi, LUO Song, LI Xi-bing. Investigation on the linear energy storage and dissipation laws of rock materials under uniaxial compression [J]. Rock Mechanics and Rock Engineering, 2019, 52(12): 4237−4255. DOI: 10.1007/s00603-019-01842-4.

[25] GONG Feng-qiang, LUO Song, YAN Jing-yi. Energy storage and dissipation evolution process and characteristics of marble in three tension-type failure tests [J]. Rock Mechanics and Rock Engineering, 2018, 51: 3613−3624. DOI: 10.1007/ s00603-018-1564-4.

[26] XIA Ying-jie, LI Lian-chong, TANG Chun-an, BAO Chun-yan, LI Ai-shan, HUANG Bo. Experiment and numerical research on failure characteristic and brittleness index for reservoir sandstone [J]. Chinese Journal of Rock Mechanics and Engineering, 2017, 36(1): 10−28. http://www.rockmech.org/CN/abstract/abstract29682.shtml. (in Chinese)

[27] ZHANG Cheng-han, YOU Shuang, JI Hong-guang, LI Fei, WANG Hong-tao. Hydraulic properties and energy dissipation of deep hard rock under H-M coupling and cycling loads [J]. Thermal Science, 2019, 23(S3): S943−S950. DOI: 10.2298/tsci18070 2181z.

[28] GOODMAN R E. Introduction to rock mechanics [M]. New York: John Wiley & Sons, 1989.

(Edited by HE Yun-bin)

中文导读

高水力条件下深部砂岩的强度与储能交互特征

摘要：为了研究围压和孔隙水压对深部砂岩强度特征、储能状态和峰值破坏时能量释放烈度的影响规律，开展一系列水力耦合条件下的三轴压缩试验。通过分析岩石变形破坏过程，获得其应力阈值。利用图形积分方法获得深部砂岩在峰前阶段总能量密度、弹性能量密度、耗散能量密度的变化趋势。对比不同围压下岩石的动态储能水平，分析孔隙水压对岩石闭合应力、起裂应力、损伤应力、峰值应力等应力阈值处能量耗散的影响。基于峰前、后总能量密度的比值，研究围压与孔隙水压对深部砂岩岩爆倾向性的相互作用机理。实验结果表明，砂岩峰值应力随着围压的增加而增加，而孔隙水压的存在可以削弱砂岩的峰值应力。在自闭合应力至峰值应力间的应力阶段，岩石的动态储能水平呈现出反“对勾”的演化趋势。同时随着围压的增加，动态储能水平上升。然而，孔隙水压增大岩石的能量耗散程度，降低岩石的储能能力，耗散程度与孔隙水压呈线性关系。围压的增大加剧深部砂岩的失稳破坏现象，而孔隙水压具有相反作用。研究成果将为高应力、高孔隙水压下砂岩地层工程岩体开挖稳定性分析提供有力的数据支撑。

关键词：深部砂岩；高水压；力学特性；能量储存；岩爆倾向性